Article

Dendrimer-Tuned Formation of Luminescent Organic Microcrystals

Franck Bertorelle, Dominique Lavabre, and Suzanne Fery-Forgues

J. Am. Chem. Soc., **2003**, 125 (20), 6244-6253• DOI: 10.1021/ja029822h • Publication Date (Web): 26 April 2003

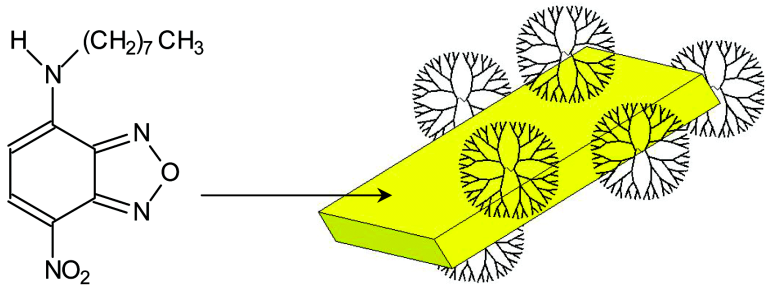

More About This Article

Additional resources and features associated with this article are available within the HTML version:

- Supporting Information
- Links to the 10 articles that cite this article, as of the time of this article download
- Access to high resolution figures
- Links to articles and content related to this article
- Copyright permission to reproduce figures and/or text from this article

View the Full Text HTML

J|A|C|S
ARTICLES
Published on Web 04/26/2003

Dendrimer-Tuned Formation of Luminescent Organic Microcrystals

Franck Bertorelle, Dominique Lavabre, and Suzanne Fery-Forgues*

Contribution from the Laboratoire des Interactions Moléculaires Réactivité Chimique et Photochimique, UMR CNRS 5623, Université Paul Sabatier, 118 Route de Narbonne, 31062 Toulouse Cedex, France

Received December 19, 2002; E-mail: sff@chimie.ups-tlse.fr

Abstract: Microcrystals of an organic fluorescent dye, 4-*n*-octylamino-7-nitrobenz-2-oxa-1,3-diazole (NBD-C8), were prepared by reprecipitation in water. The crystallization kinetics was monitored by UV/vis absorption spectroscopy, and a model was proposed. The size and shape of the microcrystals were analyzed by laser light scattering, fluorescence microscopy, and scanning electron microscopy. In the presence of PAMAM dendrimers of generation 2.5, 3.5, and 4.5, the crystallization process was drastically accelerated. The crystals obtained were smaller and more regular than those formed in pure water and were not agglomerated. There are probably two levels of interaction of NBD-C8 with the dendrimers, which act as both templates and colloid stabilizers.

Introduction

Microcrystals occupy the intermediate state between isolated molecule and bulk crystal. Therefore, they provide a unique opportunity to observe the evolution of material properties with size. Inorganic microcrystals have been extensively investigated. Fascinating properties due to quantum confinement effects have been reported for nanometer-order particles, focusing a great deal of interest on these species.[1] Since such effects were not expected for organic microcrystals, very little attention has been paid to them, mainly because of preparation difficulties. However, organic mesoscopic systems offer high diversity in their physicochemical properties, such as luminescence[2] or high nonlinear optical efficiency,[3] and they are expected to be useful as novel functional materials in electronics and photonics.[4] For this reason, the preparation and study of organic microcrystals have recently given rise to a burst of interest.[5] Moreover, understanding the laws that underlie organic particle nucleation is also important to fields such as pharmaceuticals, protein crystallization,[6] bioinspired synthesis of composite materials,[7] and biomineralization.[8]

Methods that rely on solubility changes are a convenient way to obtain organic microcrystals, the size of which is usually in the range of several tens of nanometers to sub-micrometer.[5a−i] Among them, the so-called reprecipitation method consists of first preparing a concentrated solution of the dye in a good solvent, then rapidly injecting microamounts of the solution in a poor solvent that is miscible with the first one. The good solvent disperses, and the sudden change in the surroundings of the organic compound causes its precipitation and microcrystallization.

There is an obvious lack of quantitative data concerning the reprecipitation method, especially in the initial stages. This prompted us to investigate the crystallization process of a fluorescent dye, which allowed all the steps to be studied through different techniques. The possibility to control particle size and shape was also investigated. For this, commercially available starburst dendrimers of the polyamidoamine (PAMAM) family[9] were added to the crystallization medium. These molecules are built from a nitrogen-containing core by grafting successive

(1) (a) Alivisatos, A. P. *Science* **1996**, *271*, 933−937. (b) Alivisatos, A. P.; Barbara, P. F.; Castleman, A. W.; Chang, J.; Dixon, D. A.; Klein, M. L.; McLendon, G. L.; Miller, J. S.; Ratner, M. A.; Rossky, P. J.; Stupp, S. I.; Thompson, M. E. *Adv. Mater.* **1998**, *10*, 1297−1336. (c) Michalet, X.; Pinaud, F.; Lacoste, T. D.; Dahan, M.; Bruchez, M. P.; Alivisatos, A. P.; Weiss, S. *Single Mol.* **2001**, *2*, 261−276. (d) Gerion, D.; Parak, W. J.; Williams, S. C.; Zanchet, D.; Micheel, C. M.; Alivisatos, A. P. *J. Am. Chem. Soc.* **2002**, *124*, 7070−7074.

(2) Yoshikawa, H.; Masuhara, H. *J. Photochem. Photobiol. C* **2000**, *1*, 57−78.

(3) (a) Chemla, D. S.; Zyss, J. *Nonlinear Optical Properties of Organic Molecules and Crystals*; Academic Press: Orlando, FL, 1987; Vol. 1. (b) Gehr, R. J.; Boyd, R. W. *Chem. Mater.* **1996**, *8*, 1807−1819.

(4) Oikawa, H.; Kasai, H.; Nakanishi, H. In *Anisotropic Organic Materials*; ACS Symposium Ser. 798; Glaser, R., Kasizynski, P., Eds.; American Chemical Society: Washington, DC, 2002; Chapter 12, pp 169−178.

(5) (a) Oikawa, H.; Kasai, H.; Nakanishi, H. In *Anisotropic Organic Materials*; ACS Symposium Ser. 798; Glaser, R.; Kasizynski, P., Eds.; American Chemical Society: Washington, DC, 2002; Chapter 11, pp 158−168, and references therein. (b) Nalwa, H. S.; Kasai, H.; Okada, S.; Oikawa, H.; Matsuda, H.; Kakuta, A.; Mukoh, A.; Nakanishi, H. *Adv. Mater.* **1993**, *5*, 758−760. (c) Kasai, H.; Oikawa, H.; Okada, S.; Nakanishi, H. *Bull. Chem. Soc. Jpn.* **1998**, *71*, 2597−2601. (d) Kasai, H.; Kamatani, H.; Yoshikawa, Y.; Okada, S.; Oikawa, H.; Watanabe, A.; Itoh, O.; Nakanishi, H. *Chem. Lett.* **1997**, 1181−1182. (e) Kasai, H.; Kamatani, H.; Okada, S.; Oikawa, H.; Matsuda, H.; Nakanishi, H. *Jpn. J. Appl. Phys.* **1996**, *35*, L221-L222. (f) Kasai, H.; Nalwa, H. S.; Oikawa, H.; Okada, S.; Matsuda, H.; Minami, N.; Kakuta, A.; Ono, K.; Mukoh, A.; Nakanishi, H. *Jpn. J. Appl. Phys.* **1992**, *31*, L1132−1134. (g) Onodera, T.; Oshikiri, T.; Katagi, H.; Kasai, H.; Okada, S.; Oikawa, H.; Terauchi, M.; Tanaka, M.; Nakanishi, H. *J. Cryst. Growth* **2001**, *229*, 586−590. (h) Baba, K.; Kasai, H.; Okada, S.; Oikawa, H.; Nakanishi, H. *Jpn. J. Appl. Phys.* **2000**, *39*, L1256-L1258. (i) Van Keuren, E.; Georgieva, E.; Adrian, J. *Nano Lett.* **2001**, *1*, 141−144. (j) Sanz, N.; Baldeck, P. L.; Ibanez, A. *Synth. Met.* **2000**, *115*, 229−234. (k) Akimov, I. A.; Denisyuk, I. Yu.; Meshkov, A. M. *Opt. Spektrosk.* **1994**, *77*, 954−958. (l) Fu, H.-B.; Wang, Y.-Q.; Yao, J.-N. *Chem. Phys. Lett.* **2000**, *322*, 327−332. (m) Horn, D.; Rieger, J. *Angew. Chem., Int. Ed.* **2001**, *40*, 4330−4361.

(6) Rosenberger, F.; Vekilov, P. G.; Muschol, M.; Thomas, B. R. *J. Cryst. Growth* **1996**, *168*, 1−27.

(7) Estroff, L. A.; Hamilton, A. D. *Chem. Mater.* **2001**, *13*, 3227−3235.

(8) (a) Addadi, L.; Weiner, S. *Angew. Chem., Int. Ed. Engl.* **1992**, *31*, 153−169. (b) Baeuerlein, E. *Biomineralization*; Wiley-VCH: Weinheim, 2000.

 10.1021/ja029822h CCC: $25.00

Chart 1. Chemical Structure of Compound 1

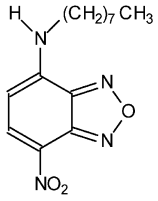

layers of amidoamine units, each of them constituting a "generation". The "half-generation" dendrimers used in this work bear an "unfinished" external layer, terminated by carboxylate groups with sodium contraions. These polyanionic assemblies have been reported to tune the crystallization of inorganics. For instance, they switch the crystallization of $CaCO_3$ toward the formation of spherical vaterite crystals, whereas rhombohedral calcite crystals are formed in their absence.[10] They have also been used to control the size of gold, platinum, and silver nanoparticles, produced by the reduction of their salts.[11] However, as far as we know, dendrimers have not been used yet for assisting the formation of organic microcrystals. Neither have they been used in the course of a reprecipitation process.

As organic dye, an amino derivative of the 7-nitrobenz-2-oxa-1,3-diazol-4-yl (NBD) group, was chosen. Compounds of this type are particularly polar, due to the presence of an amino group as an electron donor and of both a nitro group and a furazan ring which combine their electron-withdrawing effects. Their ground-state dipole moment has been calculated to be around 9 D.[12] Some derivatives have been reported to display nonlinear optical properties.[13] They are also excellent probes for UV/vis absorption and fluorescence spectroscopy, sensitive to the polarity and acidity of their environment.[14] In addition, they can be easily synthesized by NBD chloride reacting with organic amines. This is how NBD-C8 (**1**, Chart 1) was obtained. It is hydrophobic, owing to its alkyl chain that bears eight carbon atoms. In a previous paper, **1** was shown to be useful to study the interaction of a neutral probe with micelles.[15] In the present work, the crystallization of **1** in water was investigated by UV/vis absorption spectroscopy, fluorescence spectroscopy, granulometry, and microscopy. The kinetics of this phenomenon was first studied in the absence of dendrimer. Then, the 3.5 generation (G3.5) dendrimer, bearing 64 carboxylic groups at its periphery, was used at various concentrations. Finally, a comparison was made with the G2.5 and G4.5 dendrimers, terminated by 32 and 128 carboxylate groups, respectively.

(9) (a) Tomalia, D. A.; Naylor, A. M.; Goddard, W. A. *Angew. Chem., Int. Ed. Engl.* **1990**, *29*, 138−175, and references therein. (b) Zeng, F.; Zimmerman, S. C. *Chem. Rev.* **1997**, *97*, 1681−1712.
(10) (a) Naka, K.; Tanaka, Y.; Chujo, Y.; Ito, Y. *J. Chem. Soc., Chem. Commun.* **1999**, 1931−1932. (b) Naka, K.; Tanaka, Y.; Chujo, Y. *Langmuir* **2002**, *18*, 3655−3658.
(11) Esumi, K.; Suzuki, A.; Yamahira, A.; Torigoe, K. *Langmuir* **2000**, *16*, 2604−2608.
(12) Mukherjee, S.; Chattopadhyay, A.; Samanta, A.; Soujanya, T. *J. Phys. Chem.* **1994**, *98*, 2809−2812.
(13) (a) Mori, J.; Kaino, T. *Phys. Lett. A* **1988**, *127*, 259−262. (b) Suzuki, H.; Hiratsuka, H. *Proc. SPIE-Int. Soc. Opt. Eng.* **1988**, *971*, 97−106.
(14) (a) Fery-Forgues, S.; Fayet, J.-P.; Lopez, A. *J. Photochem. Photobiol.* **1993**, *70*, 229−243. (b) Lin, S.; Struve, W. S. *Photochem. Photobiol.* **1991**, *54*, 361−365. (c) Mukherjee, P.; Cardinal, J. R. *J. Phys. Chem.* **1978**, *82*, 1620−1627. (d) Chattopadhyay, A.; London, E. *Biochemistry* **1987**, *26*, 39−45. (e) Chattopadhyay, A.; London, E. *Biochem. Biophys. Acta* **1988**, *938*, 24−34. (f) Rajarathnam, K.; Hochman, J.; Schindler, M.; Ferguson-Miller, S. *Biochemistry* **1989**, *28*, 3168−3176. (g) Mukherjee, S.; Chattopadhyay, A.; Samanta, A.; Soujanya, T. *J. Phys. Chem.* **1994**, *98*, 2809−2812.
(15) Galinier, F.; Bertorelle, F.; Fery-Forgues, S. *C. R. Acad. Sci. Paris* **2001**, *4*, 941−950.

Experimental Section

Materials. Absolute ethanol was from Carlo Erba Reagenti. High-pressure demineralized water (resistivity 16 MΩ cm) was used. The 4-*n*-octylamino-7-nitrobenz-2-oxa-1,3-diazole (NBD-C8, **1**) probe was prepared as previously described,[15] according to a variant of the synthesis reported by Heberer et al.[16] PAMAM starburst dendrimers were purchased from Aldrich and used without further purification. Sodium acetate was from Prolabo. Sodium dodecanoate (sodium laurate) was from Acros.

Apparatus. UV/vis absorption spectra were recorded on a Hewlett-Packard 8452A diode array spectrophotometer. The measurements were conducted at 25 °C in a thermostated cell. The particle size was measured by using a Mastersizer S granulometer from Malvern Instruments, for the 0.05−900 μm range. Detection was based on low-angle laser light scattering, according to the Mie theory. The excitation wavelength was 633 nm. A 100 mL cell equipped with continuous stirring was used for the sample. The size and shape of the microcrystals were observed with a Zeiss MC80DX fluorescence microscope and a TEMSCAN 200CX scanning electron microscope. For TEM, a droplet of NBD-C8 (2×10^{-5} M) and dendrimer (4×10^{-5} M) aqueous solution was taken and put on a carbon grid at a given time after mixing. The excess liquid was drawn off with paper, and the sample was revealed with ammonium molybdate (2%) as a contrasting agent and allowed to dry for 12 h at room temperature. Infrared spectroscopy was performed with a Perkin-Elmer 1760-X infrared Fourier transform spectrometer using KBr pellets. The microanalyses were obtained with a EA1110 elemental analyzer from CE Instruments. Sodium was assayed on a Jobin Yvon inductively coupled plasma (ICP) spectrometer. Calibration and measurements were done at 589.6 nm, corresponding to sodium light emission.

Preparation of the Solutions. An aliquot of the commercial methanol solution of PAMAM starburst dendrimer was transferred to a 10 mL measuring flask. The methanol was evaporated off under vacuum, and the flask was filled with water. This solution (10^{-3} M) was subsequently diluted if necessary, to obtain various concentrations in dendrimer. A solution of NBD-C8 (**1**) at 10^{-3} M in absolute ethanol was prepared independently. Then, a small volume of the dye solution was introduced into the dendrimer aqueous solution. For example, for absorption measurements, 40 μL of this solution was transferred to a cell containing 1.96 mL of the dendrimer solution in water. The proportion of ethanol in water was 2% v/v for every experiment.

Determination of the Solubility Threshold of NBD-C8. The solubility threshold was measured in two different ways. With the first method, 200 μL of the dye solution (10^{-3} M) in absolute ethanol was introduced in a 10 mL measuring flask. Ethanol was evaporated off under vacuum, then the flask was filled with water containing 2% ethanol (v/v). The solution was stirred for 20 h, then filtered with a 0.2 μm Millipore filter. With the second method, 200 μL of the dye solution in ethanol was added to 10 mL of water. The solution was stirred for 20 h and filtered as previously. The dye concentration in the filtered solutions was determined by UV/vis absorption spectroscopy, using cells of 10 cm optical pathway. The two methods yielded similar results.

Absorption Data Analysis. An apparent molar absorption coefficient $\epsilon_{i(app)}$ was assigned to each species *i*. Absorbance *A* was related to concentrations C_i using the relationship $A = l\sum(\epsilon_{i(app)}C_i)$ where *l* is the optical path-length. The system of differential equations with independent variables was numerically integrated by a semi-implicit Runge−Kutta (SRK) method.[17] The sum of the squares of the differences between the experimental values and those of the numerical calculation was minimized by a Powell nonlinear minimization algorithm.

(16) Heberer, H.; Kersting, H.; Matschiner, H. *J. Prakt. Chem.* **1985**, *327*, 487−504.
(17) Kaps, K.; Rentrop, P. *Comput. Chem. Eng.* **1984**, *8*, 393−396.

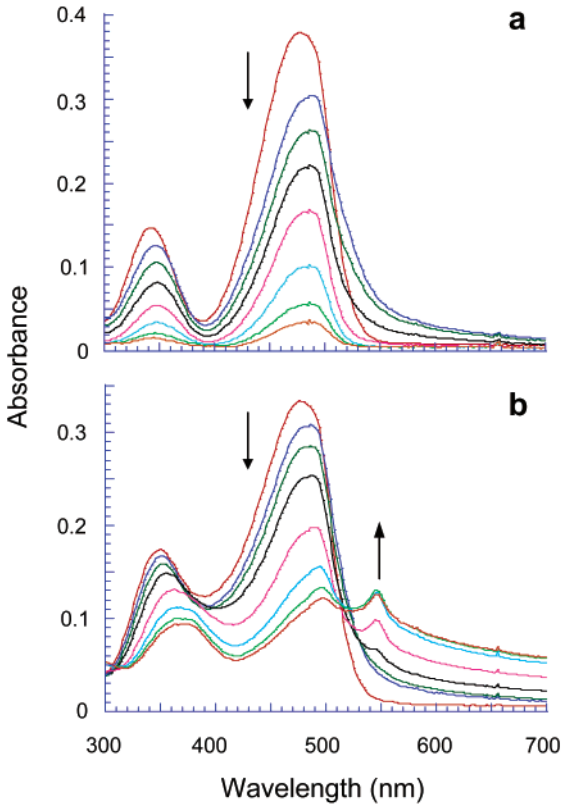

Figure 1. Evolution of the UV/vis absorption spectrum of **1** (2×10^{-5} M) in water containing 2% v/v ethanol, during the reprecipitation process: (a) in the absence of dendrimer, one measurement every 3 min; (b) in the presence of PAMAM 3.5G dendrimer (4×10^{-5} M), one measurement every min.

Results

Reprecipitation of NBD-C8 in Water in the Absence of Dendrimer. As said above, the fluorescent probe NBD-C8 (**1**) is a very hydrophobic compound. Its solubility limit in water containing 2% (v/v) ethanol was found to be around 4×10^{-7} M. For reprecipitation measurements, a small amount of a concentrated ethanol solution of dye was rapidly introduced into water under continuous stirring (see Experimental Section). The final solution contained 2% ethanol (v/v) in water and 2×10^{-5} M dye; that is, the dye concentration was 50 times higher than the solubility threshold. Just after mixing, the aqueous solution of dye was yellow. Then, the solution faded. It became entirely colorless within 1 h. A visible red deposit was formed on the stirrer, while a few big crystals floated in the bulk solution.

The precipitation process was monitored by UV/vis absorption spectroscopy. In pure ethanol, **1** displayed the characteristic spectrum of dispersed amino-NBD probes.[18] An intense charge transfer (CT) band peaked at 464 nm, accompanied by a band of moderate intensity at 332 nm, which corresponds to a $\pi-\pi^*$ transition. Immediately after introducing the ethanol solution of **1** into water, the shape of the spectrum was preserved, but the bands were shifted respectively to 476 and 344 nm (Figure 1a). In the first seconds after mixing, both bands continued shifting to the red up to 482 and 346 nm. This evolution is attributable to the progressive dispersion of ethanol in the aqueous phase and to the consequent dye solvation by the water molecules. Then, the intensity of the two bands decreased, without a subsequent shift of the maxima (Figure 1a). The widening of the CT band caused an absorbance increase above 546 nm, then the absorbance decreased after 7 min and came back to the level of the original baseline after 36 min.

Reprecipitation of NBD-C8 in Water in the Presence of Dendrimer. A procedure similar to that used above was followed to study the effect of the dendrimers upon the reprecipitation process. The concentrated solution of **1** in ethanol was added to an aqueous solution that contained G3.5 PAMAM dendrimer up to a concentration of 8×10^{-4} M. This solution lost its color up to10 times faster than when pure water was used. Almost no deposit was observed on the stirrer, and very small crystals, which made the solution blurred, precipitated slowly.

The corresponding spectroscopic effect was different from that observed in the absence of dendrimer. For instance, in the presence of 4×10^{-5} M G3.5 dendrimer, the CT band moved to 496 nm, the $\pi-\pi^*$ band was shifted to 364 nm, and a new peak appeared at 546 nm (Figure 1b). Simultaneously, the baseline moved markedly upward, due to the turbidity of the suspension.

Choice of a Model and Processing of the Spectroscopic Data. Both the intensity of the CT band and that of the $\pi-\pi^*$ band are proportional to the dye concentration and lead to the same concentration values. Therefore, we only monitored the CT band that exhibits the stronger variations and thus gives the more accurate measurements. The crystallization kinetics was analyzed at three different wavelengths, chosen to obtain maximum information: 476, 502, and 546 nm. The curves roughly displayed the same shape whether the dendrimer was present in the solution or not. The shape was unusual (Figure 2). At 476 nm, the absorption intensity first decreased abruptly, then slowed. A second steep descent was observed, after which the curve leveled off in approach to the final state. At 502 and 546 nm, the first step was an absorbance increase, instead of a decrease.

An induction period followed by an acceleration can be characteristic of autocatalysis, namely, the already-formed species induce the buildup of other species. Experimentally, autocatalysis was evidenced by adding a new aliquot of **1** at the end of the reprecipitation process, where the final species were already formed. No new induction step was observed in these conditions, and the speed was maximum as soon as the addition of **1** was completed. Moreover, the lower the concentration of **1**, the longer the induction period.

Among the different models that were investigated, the following are the simplest that resulted in a satisfactory fit.

(1) In the Absence of Dendrimer. This model considered four distinct species. Introducing two steps (II and III) of autocatalysis was necessary to fit all three curves.

$$\mathrm{A} \rightarrow \mathrm{B} \qquad r_1 = k_1[\mathrm{A}] \qquad \text{(I)}$$

$$\mathrm{B} \xrightarrow{\mathrm{C}} \mathrm{C} \qquad r_2 = k_2[\mathrm{B}](1 + k_{\mathrm{C}}[\mathrm{C}]) \qquad \text{(II)}$$

$$\mathrm{C} \xrightarrow{\mathrm{D}} \mathrm{D} \qquad r_3 = k_3[\mathrm{C}](1 + k_{\mathrm{D}}[\mathrm{D}]) \qquad \text{(III)}$$

Considering equilibria instead of simple reactions did not lead to any improvement of the fit. The following differential equation system was written:

(18) Heberer, H.; Matschiner, H *J. Prakt. Chem.* **1986**, *328*, 261−274.

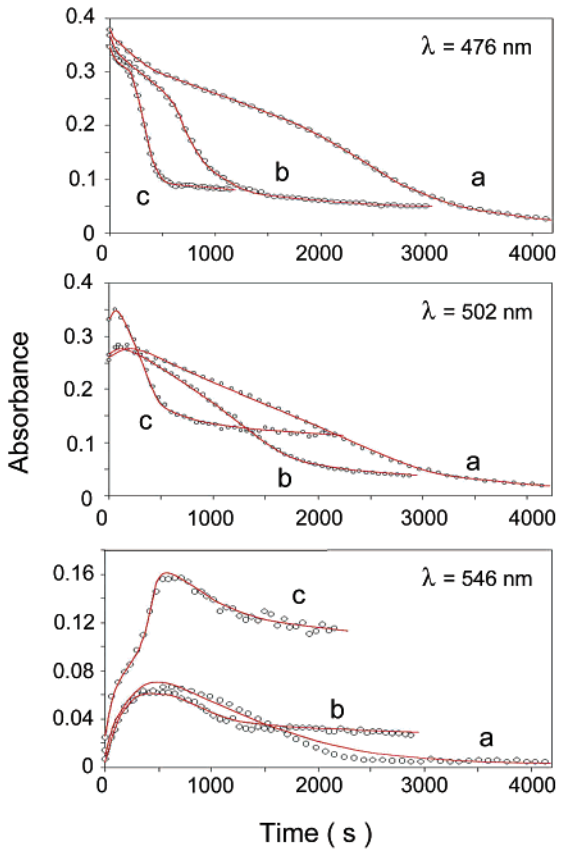

Figure 2. Kinetics of the reprecipitation process of **1** (2×10^{-5} M) monitored at 476, 502, and 546 nm in the absence of dendrimer (a) and in the presence of 6.7×10^{-6} M (b) and 5×10^{-5} M (c) PAMAM 3.5G dendrimer. The points are experimental, and the curves were calculated by the kinetics model.

$$d[A]/dt = -r_1 \quad (1)$$

$$d[B]/dt = r_1 - r_2 \quad (2)$$

$$d[C]/dt = r_2 - r_3 \quad (3)$$

$$d[D]/dt = r_3 \quad (4)$$

It must be underlined that as used here the term "species" does not refer to compounds of different chemical compositions, but of different organizational states. NBD-C8 is the only constituent of these "species", but it will be seen below that this compound can be encountered as solvated molecules, aggregates, and microcrystals. Considering distinct entities was necessary to materialize the various steps of the reprecipitation process. Moreover, these entities are spectroscopically different and characterized by their apparent molar absorption coefficients, given as Supporting Information.

(2) In the Presence of Dendrimer. In this case, the absorbance of species A was slightly decreased compared to that in water. However, this variation was weak enough to be ignored, and the same $\epsilon_{(app)}$ value was attributed to the starting species, A. The presence of dendrimer accelerated the first step of the kinetics (I′) and led to a species with spectroscopic properties that were close to those of species B obtained previously. The dendrimer also induced the formation of species C′ and D′ (steps IV and V), whose apparent absorption coefficient differed from that of species C and D. However, species C′ and D′, obtained with the assistance of dendrimer, coexisted in solution with species C and D, which formed spontaneously in water. Consequently, steps II and III were still necessary to account for the whole system. Additionally, it was necessary to consider the formation of a new species, to process all the kinetic data. Actually, in the absence of dendrimer, species D precipitated and its absorbance in the solution became negligible. In the presence of dendrimer, a proportion of species D′ remained in suspension and thus still contributed to the absorbance of the solution. This is the reason a reversible sedimentation step (VI) was added.

$$A \rightarrow B \qquad r_1' = k_1'[A] \quad (I')$$

$$B \xrightarrow{C} C \qquad r_2 = k_2[B](1 + k_C[C]) \quad (II)$$

$$C \xrightarrow{D} D \qquad r_3 = k_3[C](1 + k_D[D]) \quad (III)$$

$$B \xrightarrow{C'} C' \qquad r_4 = k_4[B](1 + k_{C'}[C']) \quad (IV)$$

$$C' \xrightarrow{D'} D' \qquad r_5 = k_5[C'](1 + k_{D'}[D']) \quad (V)$$

$$D' \rightleftarrows E \qquad r_6 = k_6[D'] - k_7[E] \quad (VI)$$

The corresponding differential equations are

$$d[A]/dt = -r_1' \quad (5)$$

$$d[B]/dt = r_1' - r_2 - r_4 \quad (6)$$

$$d[C]/dt = r_2 - r_3 \quad (7)$$

$$d[C']/dt = r_4 - r_5 \quad (8)$$

$$d[D]/dt = r_3 \quad (9)$$

$$d[D']/dt = r_5 - r_6 \quad (10)$$

$$d[E]/dt = r_6 \quad (11)$$

Constants k_2, k_3, k_C, and k_D were set identical to those previously determined in pure water. Moreover, $k_{C'}$ and $k_{D'}$ were taken equal to k_C and k_D, respectively. Experiments were carried out on 16 different dendrimer concentrations. For each experiment, fitting was performed simultaneously on the curves obtained by absorption spectroscopy at the three distinct wavelengths. Good fits were obtained in every case, as illustrated in Figure 2. The values of the calculated constants are gathered in Table 1.

The values of the rate constants k_1', k_4, and k_5 were also determined. An example is given in Table 2.

It is interesting to note that very similar steps are encountered in this kinetic system in the absence and in the presence of dendrimer. In the model used, the dendrimer was considered like a catalyst of the reprecipitation process. Plotting the values of k_1', k_4, and k_5 versus the dendrimer concentration led to a curve that raises rapidly, then levels off, meaning that a high dendrimer concentration is not necessary to obtain a significant effect on the kinetics.

It must also be underlined that the reprecipitation experiments described above were performed at 25 °C, but the same

Table 1. Values of the Constants Obtained by Processing the UV/Vis Absorption Data for the Reprecipitation of 1 (2×10^{-5} M) in the Absence and in the Presence of PAMAM G3.5 Dendrimer

k_1, s^{-1}	k_2, s^{-1}	k_3, s^{-1}	$k_C = k_{C'}$, M^{-1}	$k_D = k_{D'}$, M^{-1}	k_6, s^{-1}	k_7, s^{-1}
3.2×10^{-3}	4.6×10^{-4}	1.6×10^{-4}	1.6×10^{5}	7.2×10^{5}	3.0×10^{-4}	4.0×10^{-4}

Table 2. Values of the Rate Constants k_1', k_4, and k_5 Obtained by Processing the UV/Vis Absorption Data for the Reprecipitation of 1 (2×10^{-5} M) in the Presence of Three Different Concentrations of PAMAM G3.5 Dendrimer

[dendrimer], M	k_1', s^{-1}	k_4, s^{-1}	k_5, s^{-1}
6.7×10^{-6}	3.7×10^{-3}	1.1×10^{-3}	3.0×10^{-4}
5×10^{-5}	8.3×10^{-3}	5.2×10^{-3}	8.7×10^{-4}
5×10^{-4}	9.5×10^{-3}	7.8×10^{-3}	1.2×10^{-3}

Table 3. Values of the Rate Constants k_1, k_2, and k_3 Obtained by Processing the UV/Vis Absorption Data for the Reprecipitation of 1 (2×10^{-5} M) in the Presence of Sodium Acetate

$[CH_3COO^-Na^+]$	k_1, s^{-1}	k_2, s^{-1}	k_3, s^{-1}
4.3×10^{-4}	5.0×10^{-3}	4.7×10^{-4}	2.8×10^{-4}
3.2×10^{-3}	5.6×10^{-3}	6.1×10^{-4}	3.6×10^{-4}
2.6×10^{-2}	4.5×10^{-3}	1.3×10^{-3}	5.5×10^{-4}

experiments were also carried out at different temperatures. The whole reprecipitation process was slowed at 10 °C and accelerated at 40 °C, either in the absence or in the presence of 5×10^{-5} M dendrimer. However, at 40 °C the absorption spectrum of NBD-C8 was strongly perturbed in the presence of dendrimer. It seems that a complex process is taking place, which deserves further investigation.

Reprecipitation of NBD-C8 in Water in the Presence of Sodium Acetate. Since the dendrimers used here are polyanionic molecules, their influence upon the kinetics of dye reprecipitation could be explained by an increase in the dielectric constant of the medium. Being hydrophobic, NBD-C8 could be sensitive to this factor. To test this hypothesis, reprecipitation was carried out in the presence of sodium acetate, up to 3.2×10^{-3} M. The reprecipitation process was slightly faster than in pure water. The curves were analyzed using the model previously used for the kinetics in water, and rate constants of the same order of magnitude were obtained (Table 3). The rate of the first step was almost unchanged, but steps II and III were accelerated in the presence of increasing amounts of sodium acetate. Consequently, the dielectric constant influences the reprecipitation process. This effect was compared with that observed in the presence of dendrimer, for an identical concentration of carboxylate groups (Figure 3). It can be noted that the reprecipitation process was much slower with sodium acetate than with dendrimer. Therefore, the increase in ionic strength alone cannot account for the strong acceleration observed in the presence of dendrimer.

Laser Light Scattering. The microcrystallization process was investigated by laser light scattering (LLS). Concentrations were identical to those used for the UV/vis absorption spectroscopy measurements. However, as the stirring system was different, the kinetics obtained from the two techniques cannot be rigorously compared. Furthermore, the LLS technique does not allow the early stages of precipitation to be monitored, since it only allows detection of particles of 0.05 μm or more.

In the absence as well as in the presence of dendrimer, three distinct species of increasing size appeared successively as time

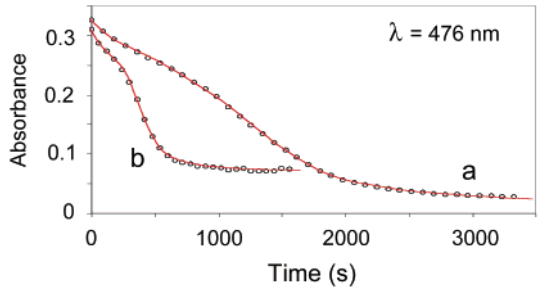

Figure 3. Kinetics of the reprecipitation process of **1** (2×10^{-5} M) monitored at 476 nm (a) in the presence of 3.2×10^{-3} M sodium acetate and (b) in the presence of 5×10^{-5} M PAMAM 3.5G dendrimer. The concentration of carboxylate groups is identical in both cases. The points are experimental, and the curves were calculated by the kinetics models.

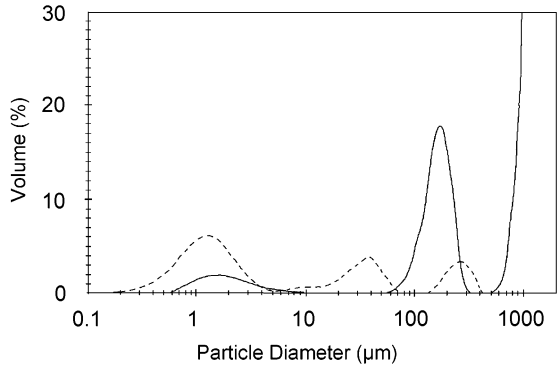

Figure 4. Diameter distribution of the NBD-C8 particles obtained by reprecipitation in water containing 2% v/v ethanol, in the absence of dendrimer after 10 min (solid line), and in the presence of 4×10^{-5} M PAMAM 3.5G dendrimer after 4 min (broken line). Total dye concentration: 2×10^{-5} M.

elapsed. It was clear that the proportion of the first species decreased while the biggest species were forming. However, marked differences were observed in the size of the particles. For pure water, their diameter was around 2 μm, 180 μm, and above 1 mm. In the presence of 5×10^{-5} M dendrimer, smaller particles appeared, their diameters being centered on 1.5, 40, and 300 μm. Figure 4 displays the different populations that coexist during the experiment.

Transmission Electron Microscopy (TEM) and Fluorescence Microscopy. The samples used for microscopy were prepared as follows. NBD-C8 was injected into a solution of PAMAM dendrimer, generation 3.5 (4×10^{-5} M), so that the final dye concentration was 2×10^{-5} M. In these conditions, crystallization was finished within 6 min. For samples taken 1.30 min after injection (see details in the Experimental Section), the TEM analysis revealed small spots, 3−5 nm in size. These spots generated no diffraction diagram, which suggests that they were made of amorphous matter. For samples taken 4 min after mixing, amorphous clusters were detected, some having the same size as before, others seeming to be 50−100 nm in diameter. They coexisted with thin rectangular structures that were about 3 μm long and 1 μm wide (Figure 5). The inset in Figure 4 is the electron diffraction pattern, which confirmed

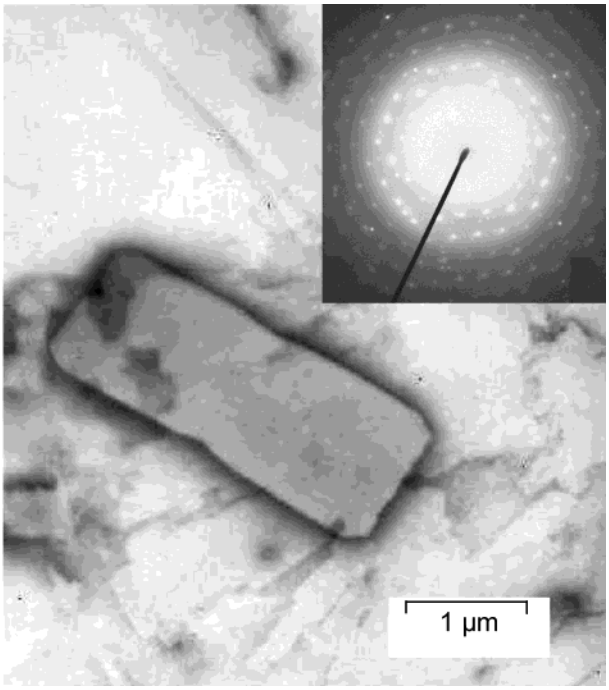

Figure 5. TEM image of NBD-C8 microcrystals obtained by the reprecipitation method in water containing 2% ethanol v/v, in the presence of 4×10^{-5} M PAMAM 3.5G dendrimer, after 4 min. The inset shows the corresponding electron diffraction pattern.

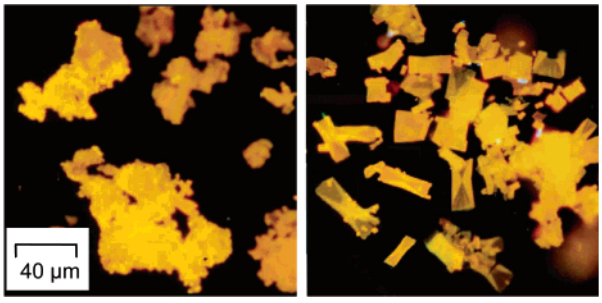

Figure 6. Fluorescence microscopy image of NBD-C8 microcrystals grown in the absence (left) and in the presence of 4×10^{-5} M PAMAM 3.5G dendrimer (right). Total dye concentration: 2×10^{-5} M; 100× magnification. The scale is the same for the two images.

that these species were crystals. Additionally, the TEM photograph showed a kind of sheet or film that did not diffract.

For fluorescence microscopy, the solution was used after crystallization was completed. Figure 6 (right) displays the fluorescence microscopy photograph of the NBD-C8 crystals, obtained in the presence of dendrimer. These regular small crystals emitted above 580 nm. They were rectangles, with slightly concave faces and an X-shaped pattern at the center. It must be emphasized that these crystals were *extremely thin* and easily remained in suspension in solution. Three populations were distinguished, with sizes 40×15, 15×8, and 4×2 μm for the two largest sides. It can be noted that the results obtained by fluorescence microscopy differed from the crystal size determined by LLS. The discrepancy found can be attributed to the fact that LLS provides an average particle diameter, while the crystals studied were very far from being spherical.

In contrast to the crystals grown in the presence of dendrimer, the crystals obtained in pure water were not monocrystals (Figure 6, left). They agglomerated and precipitated readily and did not return to suspension under stirring.

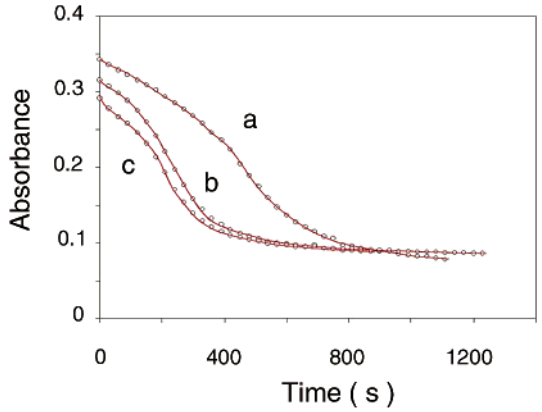

Figure 7. Kinetics of the reprecipitation process of **1** (2×10^{-5} M) monitored at 476 nm in the presence of G2.5 (a), G3.5 (b), and G4.5 (c) dendrimers (4×10^{-5} M). The points are experimental, and the curves are calculated.

Influence of the Dendrimer Size upon the Reprecipitation Process. It is conceivable that the dendrimer shape and size play a role in the preparation of NBD-C8 microcrystals. For this reason, PAMAM dendrimers of the 2.5 and 4.5 generations were used in the same experimental conditions as the 3.5 generation dendrimer. Let us recall that these dendrimers respectively bear 32, 128, and 64 carboxylic groups at their periphery. First, the G2.5 and G4.5 dendrimers were used at a concentration of 4×10^{-5} M. As previously, the reprecipitation kinetics was monitored by UV/vis absorption spectroscopy (Figure 7). The curves obtained were similar in shape to those recorded using dendrimer G3.5 and were satisfactorily fitted by the same model. However, since the presence of dendrimer G4.5 caused a marked decrease in the initial absorbance of **1**, compared with water, this effect was taken into account, and species A was attributed a slightly different $\epsilon_{(app)}$ value according to the dendrimer used. It appears that the kinetics was slower in the presence of the G2.5 dendrimer than for the dendrimers of higher generations at the same concentration. For the G2.5 dendrimer, the three constants resulting from the calculation were approximately half those obtained for the other dendrimers. In contrast, the constants were roughly similar for the G3.5 and the G4.5 dendrimers.

Then, the dendrimer concentration was set at 8×10^{-5} M for G2.5 and 2×10^{-5} M for G4.5. In these conditions, the concentration of carboxylic group was 2.6×10^{-3} M in both cases and was identical to that obtained for the 3.5 generation dendrimer at 4×10^{-5} M. The comparison of the corresponding reprecipitation kinetics showed that the curves obtained for the G3.5 and the G4.5 dendrimers were almost superimposed, while the curve obtained with the G2.5 dendrimer obviously revealed a much slower process. This confirms the results obtained in the previous section.

Interaction of Dilute NBD-C8 with PAMAM Dendrimers Studied by UV/Vis Absorption Spectroscopy. An interesting feature in Figure 7 was that the initial absorbance was slightly different according to the dendrimer used. This suggests that **1** readily interacts with the dendrimers. To get a thorough insight into the nature of this interaction, the behavior of **1** in the presence of the three dendrimers was investigated at low dye concentration (1×10^{-6} M). Although this concentration was slightly higher than the solubility limit, the solutions remained clear for many hours, and the reprecipitation process did not

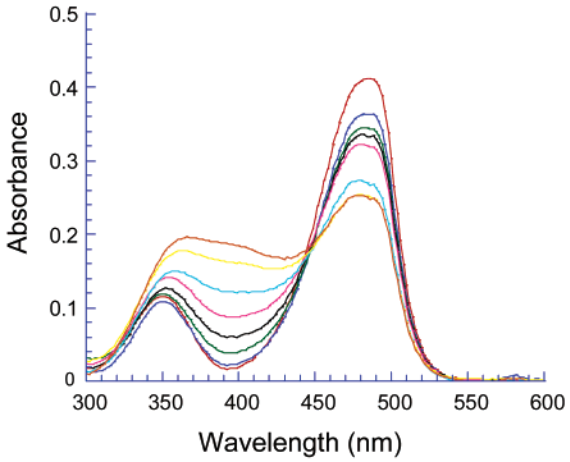

Figure 8. Evolution of the UV/vis absorption spectrum of **1** (1×10^{-6} M) in water containing 2% ethanol, in the absence and in the presence of PAMAM 3.5G dendrimer. From top to bottom at 486 nm: [dd] = 0 M; 1.7×10^{-6} M; 3.3×10^{-6} M; 5×10^{-6} M; 7.1×10^{-6} M; 1.4×10^{-5} M; 2.9×10^{-5} M; 4×10^{-5} M.

Table 4. Calculated Equilibrium Constants Related to the Interaction of 1 (1×10^{-6} M) with PAMAM Dendrimers of Three Different Sizes[a]

dendrimer	K_i([dd]), M^{-1}	K_i([COO^-]), M^{-1}
G2.5	5.5×10^4	1.7×10^3
G3.5	2.1×10^5	3.3×10^3
G4.5	4.5×10^5	3.5×10^3

[a] The absorbance variation was analyzed with respect to the dendrimer concentration [dd] or to the carboxylate group concentration [COO^-].

interfere with measurements. The dendrimer concentration ranged from 0 to 3×10^{-5} M. A small amount of dendrimer was enough to induce a significant decrease in absorbance of the CT band. Simultaneously, a wide unresolved band appeared between 360 and 420 nm. The isosbestic point was not perfect, which was attributed to successive dilutions (Figure 8). The effect was stronger for the G4.5 dendrimer than for dendrimers of lower generations.

To obtain the interaction constants, the variation in absorbance intensity at 400 and at 486 nm was plotted with respect to the dendrimer concentration and processed simultaneously. The curve obtained was satisfactorily fitted by assuming a 1:1 stoichiometry, and the fit was not improved by taking further equilibria into account. The equilibrium can be written

$$\text{NBD-C8} + \text{dd} \rightleftarrows \text{NBD-C8-dd} \qquad \text{(VII)}$$

where dd stands for the dendrimer, with the equilibrium constant K_i:

$$K_i = [\text{NBD-C8-dd}]/[\text{NBD-C8}][\text{dd}] \qquad (12)$$

The system was solved as explained elsewhere.[19] The calculated constants are reported in Table 4. It was noticeable that the binding constant for the G3.5 dendrimer was around 4 times that for G2.5, and the constant for G4.5 was about twice that for G3.5. The variation in absorbance intensity was then analyzed with respect to the concentration of carboxylate groups. The value of the equilibrium constants obtained for the G3.5 and G4.5 dendrimers was found to be quite close in all cases and higher than that obtained for the G2.5 dendrimer (Table 4).

Owing to their strongly polar nature, amino-NBD probes may interact with the dendrimer carboxylate groups through electrostatic attractive forces. To test this hypothesis, the effect of adding sodium acetate on the absorption spectrum of dilute **1** (1×10^{-6} M) was investigated. In this case, a decrease in absorbance intensity at 486 nm was actually observed, though no variations were detected at shorter wavelengths. It can be noted that large amounts of salt (up to 7.5×10^{-1} M) were needed to obtain a significant spectroscopic effect. A very weak equilibrium constant (40 M^{-1}) was obtained by processing the data at 486 nm. The absorbance decrease at 486 nm can thus be assigned to an interaction between **1** and the carboxylate group. However, the spectroscopic effect observed with the dendrimers was much stronger. The difference by 2 orders of magnitude in the value of the constants obtained with sodium acetate and with the dendrimers also indicates that an additional stabilization occurs in the latter case. Actually, it is known that ionic dyes can bind at the surface of oppositely charged dendrimer.[20] The same could happen for NBD probes, which might not be ionic but at least are strongly polar.

Interaction of Dilute NBD-C8 with PAMAM Dendrimers and Anionic Micelles Studied by Fluorescence Spectroscopy. Fluorescence spectroscopy was used to corroborate the hypothesis that the interaction with the dye was taking place at the periphery of the dendrimer. In water, the emission maximum of **1** (5×10^{-7} M) was 560 nm. A shift of only 2 nm toward the blue was detected in the presence of 2.5G, 3.5G, and 4.5G dendrimers up to 10^{-3} M. This result points out that the polarity of the probe environment was almost unchanged; hence the NBD head was not inserted within the dendrimer structure, the latter being compact or not. However, this does not preclude that the alkyl chain of **1** anchors the probe within the dendrimer structure. Evidence for this is presently being sought, using NBD probes that bear alkyl chains of different lengths.

For the sake of comparison, **1** (5×10^{-7} M) was placed in the presence of sodium dodecanoate (6.4×10^{-2} M), at a concentration higher than the critical micellar concentration (2.4×10^{-2} M at 25 °C).[21] The absorption maximum was 480 nm, and the emission maximum was 545 nm, shifted by 15 nm to the blue by comparison with the fluorescence maximum in water. When increasing the dye concentration up to 2×10^{-5} M in the micellar medium, no precipitation was noted. This behavior is strongly reminiscent of that observed with **1** in the presence of other micellar systems.[15] It was attributed to the incorporation of the probe into micelles, where it was located in the interfacial region. This behavior is totally different from that encountered in the presence of dendrimers. Overall, these results support the fact that **1** is not entrapped within the dendrimer.

Composition of the Microcrystals Grown in the Presence of Dendrimer. Another point was whether a hybrid material was formed between the dendrimer and the NBD-C8 microcrystals. Therefore, microcrystals grown in the presence of 3.5G dendrimer (5×10^{-5} M) were collected, carefully rinsed with

(19) Dondon, R.; Fery-Forgues, S. *J. Phys. Chem. B* **2001**, *105*, 10715−10722.

(20) Jockusch, S.; Turro, N. J.; Tomalia, D. A. J. *Inf. Recording* **1996**, *22*, 427−433.

(21) Fendler, J. H.; Fendler, E. J. *Catalysis in Micellar and Macromolecular Systems*; Academic Press: London, 1975; p 20.

water, and dried under vacuum. They were compared to crystals grown in water alone, drained, and dried in the same way. The Fourier transform infrared spectrum of the two sets of crystals was identical. The characteristic peaks of the dendrimer at 1642, 1569, and 1404 cm^{-1} were not detected. The elemental composition analysis of crystals grown in water indicated the presence of about 1.3% water (for $C_{14}H_{20}N_4O_3$, calc C, 57.53; H, 6.85; N, 19.17, found C, 56.82; H, 6.98; N, 18.91). The elemental composition of crystals grown in the presence of dendrimer was found to be C, 54.93; H, 6.33; N, 17.94. The calculated values for the dendrimer are C, 45.90; H, 6.19; N, 13.22, for $C_{494}H_{800}N_{122}O_{188}Na_{64}$. Assuming that the two sets of crystals contain an identical amount of water, the amount of dendrimer remaining in the second set can be estimated to be around 17% in weight. This corresponds to 1 mole of dendrimer for 216 mol of NBD-C8. This is in line with the quantitation of sodium obtained by inductively coupled plasma (ICP) analysis. It was checked on a mixture of **1** with PAMAM 3.5G dendrimer that this amount of dendrimer is hardly detectable by IR spectroscopy. It is tempting to denote these microcrystals as composites of NBD-C8 and dendrimer. However, the term composite must be taken in a very wide sense, since the exact arrangement of NBD-C8 molecules with respect to the dendrimer is unknown.

Discussion

Microcrystallization in the Reprecipitation Method. By processing the UV/vis absorption data collected during reprecipitation in the absence of dendrimer, we revealed a three-step mechanism, two of which were autocatalyzed. It was necessary to consider four distinct "species", this term referring to the various forms dye **1** can occur in. Let us now try to identify each of these steps and "species".

Concerning the reprecipitation process, it is generally accepted that introducing a concentrated organic solution in an aqueous medium results in the formation of fine droplets.[5a−h] Then, the solvent disperses in the bulk water. Actually, in our experimental conditions, after the ethanolic solution of **1** had been introduced in the water, the dispersion of ethanol molecules was not instantaneous. The first change of surroundings around the NBD-C8 molecules lasted around 2 s after mixing and was responsible for the progressive red shift in the UV/vis absorption spectrum. It must be noted that a spectrum identical to that obtained in pure water was measured for mixtures containing up to 10% ethanol in water. Therefore, the spectroscopic changes observed after mixing correspond to the approach of water around **1**, although the immediate environment of the dye molecules could be richer in ethanol than the bulk phase. This is supported by the result of a previous work, where we reported evidence that a strong 1:1 interaction can occur between *n*-propylamino-NBD and ethanol.[14a] We called species A the molecules of **1** in ethanol-rich surroundings. Their absorption spectrum did not indicate self-association. They are present in the solution when the first kinetics measurements are made.

During the first step of the kinetics, the ethanol-rich environment is progressively replaced by a complete water shell. This solvation process could be a key factor in the first step. The dye exposed to a poor solvent is now ready to aggregate. According to the literature, this step leads to the formation of amorphous cluster-like particles, having a range of sizes. The nucleation theory indicates that the viability of clusters generated in a supersaturated phase depends on their size.[22] Aggregation is energetically favorable, while the introduction of an interface is unfavorable, so there is a balance between the two processes. In the present case of reprecipitation, the equilibrium must be very strongly shifted toward the formation of the aggregates, because **1** is poorly soluble in water. Consequently, species B can be identified as small aggregates, such as those observed by TEM on samples taken 1.30 min after mixing (according to our kinetic scheme, B is by far the predominant species at this time).

Scheme 1. Model of Simplified Microcrystallization Process of NBD-C8 in the Reprecipitation Method: Dye 1 in Ethanol-Rich Environment (A), Small Amorphous Particles (B), Big Amorphous Particles with Germs of Crystallization (C) and Microcrystals (D)

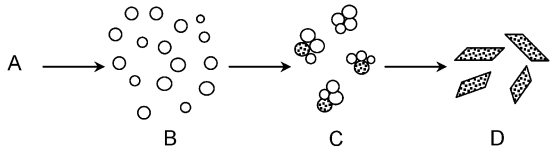

Crystallization may proceed differently according to the type of organic compound investigated. A germ of crystal can appear in amorphous particles.[5a,c] Alternatively, nucleation and crystal growth can proceed through collisions between the clusters.[5a] These processes finally lead to crystals, which are symbolized here by species D. These crystals were observed by TEM, fluorescence microscopy, and laser light scattering. It must be noted that UV/vis absorption spectroscopy cannot distinguish between the three populations of crystals that were detected by granulometry.

However, another species, called C, was necessary to process the kinetics data. At the moment, there is no physical proof that can help elucidate the identity of this species, but it can be assumed that C is an intermediate between the small aggregates B and the microcrystals D. So, species C could occur as big amorphous particles, formed by the assembly of the fine particles B, as proposed in the literature.[5a] Such large aggregates were visible by TEM in samples taken 4 min after mixing. Scheme 1 pictures the whole microcrystallization process.

It is now understandable that steps II and III are autocatalyzed. Step II is quite reminiscent of the aggregation mechanism of bacteriochlorophyll molecules, which requires the formation of a "critical" aggregation nucleus from which the larger aggregates grow.[23] In step III, the already-formed microcrystals are thought to act as a kind of template, adsorbing the amorphous particles to grow. Scanning electron microscopy actually revealed that microcrystals and amorphous particles coexist after reprecipitation, as proposed by Onodera et al.[5g]

Influence of the Dendrimer upon the Crystallization of NBD-C8. The model used to describe the reprecipitation process in pure water was very close to that used in the presence of dendrimer. However, to write this latter model, it was necessary to make a distinction between the species formed via the interaction with the dendrimer (C′ and D′) and those formed without this interaction (C and D). The species stemming from the two pathways have distinct but close spectroscopic properties

(22) (a) Davey, R. J.; Blagden, N.; Righini, S.; Alison, H.; Quayle, M. J.; Fuller, S. *Cryst. Growth Des.* **2001**, *1*, 59−65, and references therein. (b) Oxtoby, D. W. *Acc. Chem. Res.* **1998**, *31*, 91−97.
(23) Balaban, T. S.; Leitich, J.; Holzwarth, A. R.; Schaffner, K. *J. Phys. Chem. B* **2000**, *104*, 1362−1372.

(see Supporting Information), which suggest that they could slightly differ in size. The results of light scattering and fluorescence microscopy, concerning the D and D′ species, support this hypothesis. It must then be kept in mind that, qualitatively, only four types of entities were distinguished, that is, the solvated molecules (A), the small (B) and big (C and C′) aggregates, and the microcrystals (D and D′). Let us now see what type of interaction can take place between the dendrimer and the dye.

Dendrimers are highly functionalized hyperbranched polymers. Except for the low-generation dendimers, they are roughly spherical in shape, densely packed at the exterior, and somewhat hollow in the interior. In the present case, their surface bears a large number of anionic groups. Consequently, they offer different sites that can potentially interact with the NBD molecules.

The UV/vis absorption behavior showed that a strong interaction takes place between the polar NBD groups and the carboxylate groups. There is obviously a dendrimer effect, because the interaction is much stronger with the dendrimer than with sodium acetate. This indicates that the interaction can involve more than one carboxylate group per NBD-C8 molecule. As a matter of fact, at least two sites in this type of amino-NBD molecule can donate or accept hydrogen bonding. These are respectively the amino group which bears a very acidic proton (pK_a reported to be ca 9.7−10.3 in buffered aqueous methanolic solutions)[16] and the strongly negative oxygen atoms of the nitro group.[14g] The interaction with the dendrimer is probably electrostatic in nature and takes place at the dendrimer periphery. It could be imagined that a certain amount of dye is also entrapped within the dendrimer. However, the fluorescence study revealed that this is not the case, contrary to what is observed with sodium dodecanoate micelles.

Let us now turn our attention toward the way the dendrimer can accelerate the dye reprecipitation process. It was checked that the increase in dielectric constant due to the presence of the charged dendrimer cannot alone explain the effects observed. The dendrimer has an influence on every step of the kinetics. In the initial stage, the dye molecules are surrounded by an ethanol-rich phase. The solvation shell of **1** progressively becomes poorer in ethanol, and the dye exposed to water precipitates. One possibility is that the dendrimer enhances the diffusion rate of ethanol in water. This would accelerate solvent mixing and consequently the dye precipitation rate. This supposes that the dendrimer has a particular affinity for ethanol, although it is poorly soluble in this solvent. More likely, since the dendrimer has an affinity for the dye, it may compete with the ethanol molecules to establish an interaction with **1**. Another consequence of the interaction that was shown to take place between **1** and the dendrimer is that the NBD probes could arrange in order at the surface of the dendrimer (Scheme 2, top). It has been reported that this occurs for ionic dyes that form aggregates perpendicular to the dendrimer surface.[20] In our case, the molecular ordering could also be the starting point of aggregation. These two hypotheses are in total agreement with the fact that the dendrimer catalyzes the first step of the kinetics. They are also in line with the fact that above a certain dendrimer concentration, no increase in the reprecipitation rate was observed. Only a small amount of dendrimer is necessary for the formation of the embryo cluster.

Scheme 2. Top: Schematic Illustration of NBD-C8 Probes Interacting with the Dendrimer carboxylate groups. Bottom: Dendrimers Surrounding a Colloid of NBD-C8

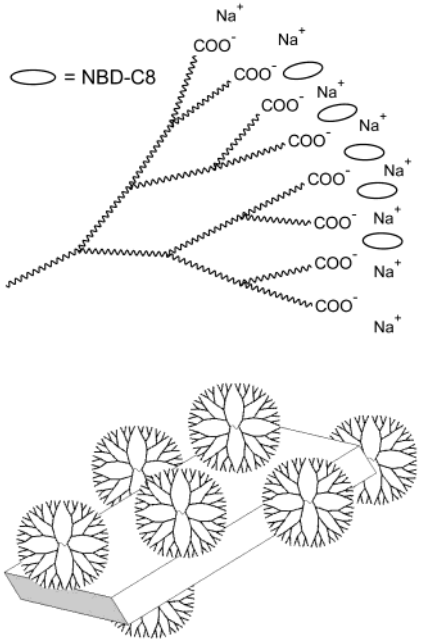

However, if the template effect at the dendrimer surface were the only one to be involved, the dendrimer would have no influence upon the subsequent steps. As a matter of fact, this was not the case, which suggests that a second phenomenon was taking place. It can be recalled that fluorescence microscopy and granulometry revealed that small crystals, and essentially monocrystals, were formed in the presence of dendrimers. This suggests that the dendrimers prevent the microcrystals from agglomerating. This hypothesis is supported by the following observation. Crystals of **1** were grown in the presence of dendrimer. After centrifugation, they readily went back into suspension in their native solution under stirring. In contrast, when the dendrimer-containing supernatant was removed and the precipitate rinsed with pure water, the crystals formed agglomerates and could not be dispersed in water again. Indirect evidence was also obtained that the dendrimers play a protective role around the microcrystals of **1**. Small crystals of **1** were grown in the presence of 4×10^{-5} M 3.5G dendrimer, then diluted NaOH was added to the suspension to pH 9. In these conditions, the crystals responded poorly to the basic attack that usually yields the hydroxyl derivative of NBD.[18,24] In comparison, the big crystals formed in pure water were readily hydrolyzed. Rinsing crystals of **1** with water eliminated a proportion of the dendrimer in the presence of which they were formed. The reactivity of the rinsed crystals was then close to that of the crystals formed in pure water. Consequently, it can be imagined that a certain amount of dendrimers arrange around the colloids of **1** (aggregates or small microcrystals) and interact with them by electrostatic forces. They form an ionic shell around the colloids (Scheme 2, bottom), thus impeding them from coalescing. It must not be forgotten that the dendrimers are much smaller than the microcrystals. Regarding the dendrimer which is still present in the rinsed crystals, X-ray studies are presently underway to determine whether the dendrimer is adsorbed at the exterior or is part of the crystal structure.

(24) Fery-Forgues, S.; Lavabre, D.; Lozar, J. *New J. Chem.* **1995**, *19*, 1177−1186.

The two hypotheses that we put forward regarding the role of the dendrimer are consistent with the dendrimer size effect that was observed. Caminati et al.[25] have reported from a fluorescence study that the PAMAM dendrimers pass from an open, branched structure for generations 0.5−3.5, to a globular compact geometry for higher generations. Consequently, the surface groups of the dendrimers are also closer to each other when the dendrimer size increases. This explains that the higher generation dendrimers were more efficient than the G2.5 dendrimer at interacting with the polar NBD-C8 molecules, at bringing them nearer, and interacting electrostatically with the colloids. However, no significant difference was found in the kinetics obtained in the presence of the G3.5 and the G4.5 dendrimer, which suggests that, from a certain size, the dendrimers have comparable effects.

The literature is of little help, because to our knowledge, the control of organic crystal growth by dendrimer has never been reported. However, an interesting comparison can be made with inorganic compounds. Precious-metal salts are generally placed in the presence of dendrimers, then submitted to chemical reduction to generate metal nanoparticles. It has been shown that the salts can enter the cavities inside a high-generation dendrimer and give rise to nanoclusters which remain entrapped within one single organic structure.[26] In other examples, much larger colloids can be stabilized by numerous dendrimers, which arrange around them by sorbing to their exterior.[11,26b,27] In the latter case, it is shown that the dendrimers offer very effective protection against nanoparticle agglomeration. This is in line with our results. It must be noted that nanocomposites are frequently formed between dendrimers and inorganic colloids, because strong interactions are involved.

Conclusion

A model describing the formation of micro- and nanocrystals could be of great interest for the paint, latex, and pharmaceuticals industries, to name just a few. By using a dye, the initial stages of nucleation and growth of organic molecular microcrystals were optically characterized here. The model we proposed seemed to be the most appropriate to take into account both the kinetics data and the observation of the colloids formed. It would be interesting to check our hypothesis using a technique that differs from UV−vis absorption spectroscopy, but which could similarly allow on-line experiments to be performed.

It was shown for the first time that anionic dendrimers can tune the formation of organic microcrystals. The use of dendrimers can contribute to the improvement of the fabrication of synthetic materials. Besides, it must not be forgotten that these dendrimers are good models for polyanionic assemblies, such as proteins, some of them being acknowledged to direct biomineralization processes.[8a,28] Understanding the role played by such templates may help solve many serious pathological problems where mineralization is involved.

Finally, the NBD-C8 particles formed can be interesting as novel materials themselves. Their luminescence and nonlinear optical properties are presently being studied. It is now clear that the experimental conditions can be markedly improved. For instance, monocrystals in the hundreds of nanometer size were obtained by using more hydrophobic probes of the same series. Work is also underway to see if the presence and the nature of the dendrimer can affect the crystallization mode. For instance, dendrimers that bear cationic or neutral groups at their periphery are under investigation.

Acknowledgment. Mr. Bertrand Floure (Malvern Instruments, Labège) is gratefully acknowledged for performing the particle size measurements.

Supporting Information Available: Apparent molar absorption coefficient for the different species in the absence and in the presence of PAMAM 3.5G dendrimer. This material is available free of charge via the Internet at http://pubs.acs.org.

JA029822H

(25) Caminati, G.; Turro, N. J.; Tomalia, D. A. *J. Am. Chem. Soc.* **1990**, *112*, 8515−8522.
(26) (a) Zhao, M.; Crooks, R. M. *Adv. Mater.* **1999**, *11*, 217−220. (b) Esumi, K.; Nakamura, R.; Suzuki, A.; Torigoe, K. *Langmuir* **2000**, *16*, 7842−7846.
(27) Garcia, M. E.; Baker, L. A.; Crooks, R. M. *Anal. Chem.* **1999**, *71*, 256−258.
(28) Banfield, J. F.; Welch, S. A.; Zhang, H.; Ebert, T. T.; Penn, R. L. *Science* **2000**, *289*, 751−754.